Growth of a Bismuth Thin Film on the Five-fold Surface of the Icosahedral Ag-In-Yb Quasicrystal

S. S. Hars[a], H. R. Sharma[a,*], J. A. Smerdon[b], S. Coates[a], K. Nozawa[c], A. P. Tsai[d], R. McGrath[a]

[a] *Surface Science Research Centre and Department of Physics, The University of Liverpool, Liverpool L69 3BX, UK*
[b] *Jeremiah Horrocks Institute for Maths, Physics and Astronomy, University of Central Lancashire, Preston PR1 2 HE, UK*
[c] *Department of Physics and Astronomy, Kagoshima University, Korimoto, Kagoshima 890-0065, Japan*
[d] *Institute of Multidisciplinary Research for Advanced Materials, Tohoku University, Sendai 980-8577, Japan*

Abstract

We present a study of growth of quasicrystalline bismuth (Bi) thin films on the five-fold surface of the icosahedral Ag-In-Yb quasicrystal using scanning tunnelling microscopy (STM). The main building block of the Ag-In-Yb quasicrystal is a rhombic triacontahedral (RTH) cluster, which is formed by successive shells of atoms. The surface is formed at bulk planes which intersect the centres of the RTH clusters. We show that the deposited Bi atoms occupy vacant sites above the surface where the atoms of the RTH clusters would be and thus Bi grows with three-dimensional quasicrystalline order. Further deposition of Bi yields crystalline Bi islands aligned along high symmetry directions of the substrate.

Keywords: Quasicrystals, Surfaces, Thin Films, Scanning Tunnelling Microscopy, Bismuth

*Corresponding author
Email address: H.R.Sharma@liverpool.ac.uk (H. R. Sharma)

1. Introduction

Quasicrystals show long-range order with a lack of translational symmetry and often possess classically forbidden rotational symmetries such as five-fold and ten-fold. Quasicrystalline phases were first observed in intermetallic compounds [1] and then in other materials such as liquid crystals [2], polymers [3, 4], colloids [5, 6], and perovskite thin films [7]. Surfaces of the intermetallic quasicrystals have provided novel templates to grow thin films of materials because of their unique five-fold and ten-fold rotational symmetry and the existence of a wide range of non-degenerate adsorption sites in comparison with conventional crystals [8, 9, 10, 11].

One of the motivations for using quasicrystals as substrates is to produce artificial structures such as single element quasicrystalline films, which will have a reduced chemical complexity compared to the bulk quasicrystals. The study of such single element quasicrystalline films will potentially play a crucial role in understanding the influence of quasiperiodicity on the physical properties of quasicrystals. For this purpose, growth of various elements on different quasicrystal surfaces has been studied using different surface techniques [9, 10, 11]. The substrates used have mostly been Al-based quasicrystals, such as the icosahedral (i)-Al-Pd-Mn and i-Al-Cu-Fe quasicrystals, or the decagonal (d)-Al-Ni-Co. Recently, the study has been extended to an Ag-based quasicrystal, namely i-Ag-In-Yb [12], which is structurally different from the Al-based quasicrystals. The structure of the Al-based quasicrystals can be explained by the pseudo-Mackay and Bergman-type clusters [13], while the Ag-based quasicrystals are formed by Tsai-type clusters, also known as the rhombic triacontahedral (RTH) clusters [14]. We will discuss the RTH clusters later.

A limited number of elements are found to grow epitaxially with quasicrystalline order on quasicrystal surfaces. The structure of the quasicrystalline thin films can be categorized into three groups: quasicrystalline monolayer films (QC ML), Fibonacci modulated films of multilayers (Fibonacci MML) and three-dimensional quasicrystalline films (3D QC). These results are summarized in

Table 1. In the QC ML films, quasicrystalline order of the adsorbate is limited up to one atomic layer [15, 16, 17, 18]. After completion of the monolayer, the adsorbate develops its natural periodic structure [19, 20, 21]. In Fibonacci MML films, the adsorbate yields atomic rows spaced in a Fibonacci sequence at coverages above a few atomic layers [22, 23]. No order is observed at lower coverage. The structure within the atomic rows is periodic. The Fibonacci MML structure of, for example, Cu/*i*-Al-Pd-Mn, is described as a vicinal surface of body-centered tetragonal Cu [24]. In the 3D QC films, the adsorbate atoms occupy the positions of vacant atoms in the truncated clusters of the bulk and thus form a three dimensional quasicrystalline film [12]. There are a few other systems which adopt the pentagonal symmetry of the substrate at submonolayer coverage such as the starfish structure of Al on *i*-Al-Pd-Mn [25] and Si on the same substrate [26]. Beyond sub-monolayer coverage the film does not grow with quasicrystalline order in these cases.

The first quasicrystalline monolayer film was reported by Prof Reider's group at Free University Berlin in 2002 [15]. Using elastic helium atom scattering (HAS) and low energy electron diffraction (LEED), it was demonstrated that Bi and Sb deposited on the five-fold surface of *i*-Al-Pd-Mn and the ten-fold surface of *d*-Al-Ni-Co form a quasicrystalline monolayer. The growth was carried out at high temperatures such that no multilayer could adsorb on the surface. The formation of quasicrystalline Bi was later confirmed by STM [18] and density functional theory (DFT) calculations [27]. These studies gave an insight into the mechanism of growth of quasicrystalline Bi. The deposited Bi first nucleates in pentagonal stars on pseudo-Mackay clusters truncated at the surface plane, forming a quasiperiodic framework. Subsequent adsorption of Bi atoms result in the formation of a quasicrystalline monolayer. After completion of a monolayer, periodic islands with specific heights (magic heights) are formed due to the quantum size effect of the islands [19]. The islands are aligned along high symmetry directions of the substrate forming a five-fold or ten-fold twinned structure [20, 21]. The structure of the islands is pseudocubic or pseudohexagonal, depending on the rate of deposition and coverage [21].

Table 1: List of quasicrystalline thin films of three different types: quasicrystalline monolayer films (QC ML), Fibonacci modulated films of multilayers (Fibonacci MML) and three-dimensional quasicrystalline films (3D QC). 5f: five-fold and 10f: ten-fold.

Structure Type	Adsorbate	Substrate	Techniques [References]
QC ML	Bi	5f-*i*-Al-Pd-Mn	LEED, HAS [15]
			ab initio [27], STM [18]
		10f-*d*-Al-Ni-Co	LEED, HAS [15], STM [28]
	Sb	5f *i*-Al-Pd-Mn	LEED, HAS [15]
		10f *d*-Al-Ni-Co	LEED, HAS [15]
	Pb	5f *i*-Al-Pd-Mn	LEED, STM [17]
	Sn	5f *i*-Al-Cu-Fe	STM [16]
	Ag	5f *i*-Al-Pd-Mn	STM [29]
Fibonacci MML	Cu	5f *i*-Al-Pd-Mn	STM, LEED, MEIS [22, 30, 31]
	Co	5f *i*-Al-Pd-Mn	STM, LEED [23]
		10f *d*-Al-Ni-Co	STM, LEED [23]
3D QC	Pb	5f *i*-Ag-In-Yb	STM, XPS, and DFT [12]
	Bi	5f *i*-Ag-In-Yb	STM [This work]

In this work, we present the growth of Bi on the five-fold surface of the *i*-Ag-In-Yb quasicrystal. Unlike on the Al-based quasicrystals, Bi on this substrate grows in quasicrystalline order beyond a monolayer. Bismuth atoms occupy the vacant sites of the truncated bulk clusters. The result is similar to Pb on the same substrate. However, the specific adsorption process differs to that for Pb.

2. Experimental Details

The Bridgman method was used to grow a single grain *i*-$Ag_{42}In_{42}Yb_{16}$ quasicrystal sample. The sample was then cut perpendicular to the five-fold axis. Prior to insertion into ultra high vacuum (UHV), 6 μm, 1 μm and 0.25 μm grades of diamond paste were used to polish the sample. Following polishing with each paste, the sample was immersed in an ultrasonic bath for 15 minutes to remove residual paste. Once the sample was inserted into the UHV chamber, it underwent repeated cycles of sputtering by Ar^+ ions (2.5 – 3 keV) for 30 minutes and subsequent annealing at a base pressure of 2×10^{-10} mbar. A Minolta LAND Cyclops 241 optical pyrometer was used to measure an annealing temperature at the sample surface of 440 °C. The emissivity of the pyrometer was set to 0.35, following a previous experiment on the same surface [32]. The annealing time for each cycle was 2 – 4 hours. This preparation resulted in a step-terrace structure with quasicrystalline order.

An Omicron EFM-3 electron beam evaporator was used to deposit Bi at room temperature with constant flux of 120 nA measured by the evaporator. The pressure was kept close to the base pressure during deposition. An Omicron variable temperature scanning tunnelling microscope was employed to characterise the surface and the epitaxial films using constant current mode at room temperature. Tunneling parameters for each STM image are given in the relevant figure captions. The stated bias voltage refers to the potential applied to the sample relative to the tip.

3. Results

The *i*-Ag-In-Yb quasicrystal has the same structure as the binary *i*-Cd-Yb phase, where Cd is replaced by Ag and In. The atomic structure of this system has been understood without ambiguity [14], in contrast to the Al-based quasicrystals [33]. The basic building block of this system, the RTH cluster, consists of five successive atomic shells, which are shown in Fig. 1(a). There are a few Yb atoms in the interstices between RTH clusters. These atoms are called 'glue atoms'.

The surface prepared under conditions explained in Section 2 yields atomically flat terraces. The terraces are formed at bulk planes intersecting the centres of the RTH clusters. The structure of such a plane is shown in Fig. 1(c). The structure can be mapped by a Penrose P1 tiling with vertices located at the centres of the clusters. The Penrose P1 tiling consists of four different tiles: pentagons of two orientations (we will refer to these as 'up-pentagon' and 'down-pentagon'), stars, rhombi and boats. The edge length of the tiling is 2.53 nm, which is τ times larger than the minimum distance between the cluster centres ($\tau = 1.618\ldots$ is an irrational number characteristic of pentagonal symmetry). The minimum distance is equivalent to the size of the RTH cluster (1.56 nm). The vertices of the tiling are uniquely decorated. The central ring of ten Cd (Ag/In) atoms corresponds to the cross-section of the fourth shell of the RTH clusters (1 (b)). The Ag/In-ring is surrounded by ten Yb pentagons which belong to the third shell or glue atoms. The Ag/In rings appear as protrusions in STM at negative bias voltage to the surface (Fig. 1(d)) [34]. However, at positive bias the Yb-rings are resolved instead of the protrusions [35]. As expected from the bulk structure, the protrusions in STM are located at the vertices of a Penrose P1 tiling of edge length 2.50 ± 0.02 nm [34].

Bismuth was gradually deposited on the surface. Fig. 2(a) shows a STM image of 20 nm × 20 nm after depositing Bi for 5 minutes. The coverage of Bi, which is estimated by subtracting the area covered by Bi atoms from the area of the structure, is about 0.35 ± 0.02 ML. The area of STM image used

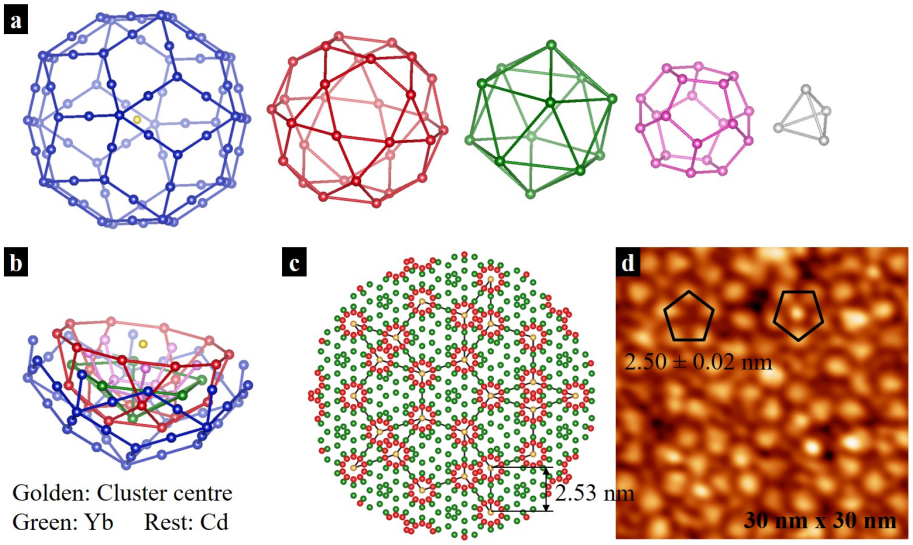

Figure 1: (a) The atomic shells of the rhombic triacontahedral (RTH) cluster, which are the building block of the *i*-Cd-Yb quasicrystal [14]. Atoms of different shells are coloured differently. In *i*-Ag-In-Yb, Cd is replaced by Ag and In. (b) An RTH cluster truncated by the surface plane. (c) In-plane atomic structure of a bulk plane, which cuts the RTH centre, where the terraces are formed. A Penrose P1 tiling of edge length 2.53 nm is superimposed. (d) STM image of the five-fold *i*-Ag-In-Yb surface showing pentagonal protrusions of 2.50 ± 0.02 nm edge length. Bias voltage, V_B = - 1.0 V, and tunneling current, I_T = 0.2 nA.

to estimate the coverage was 2500 nm^2. Clean surface protrusions and single Bi atoms are resolved at this coverage. This helps to identify the adsorption sites of Bi atoms. Individual Bi atoms appear as brighter dots in the image. Bi atoms form pentagons of 0.95 ± 0.05 nm edge length. Some of them are highlighted in Fig. 2(a). Bi pentagons have identical orientations, parallel to the orientation of the up-pentagons of the substrate. From the size, orientation and location of the Bi pentagons, adsorption sites are suggested to be between the Ag/In ring and the Yb ring around the cluster centre. These adsorption sites are marked by blue spheres in Fig. 2(b).

Most of the observed Bi pentagons at 0.35 ML coverage are incomplete. Further deposition of Bi completes these pentagons. Fig. 2(c) is an STM image of 20 nm × 20 nm, showing complete pentagons of Bi atoms. The estimated coverage is 0.56 ± 0.02 ML. In addition to the complete Bi pentagons two other features were observed at this coverage: pentagonal stars of 0.60 ± 0.01 nm edge length and crescent shapes. The crescents develop by adsorption of atoms at the edges of the Bi pentagons. A star and a crescent are highlighted in bottom of Fig. 2(c). Observed stars have two different orientations, rotated by 36° with respect to each other, and they are marked in Fig. 2(c). Many of the pentagonal stars are incomplete. The orientations of the stars reflects the orientations of up- and down-pentagons of the clean surface. The height of Bi atoms at this coverage is 0.12 ± 0.01 nm from the substrate (Refer to the line profile shown in Fig. 2(a), bottom). We refer to the network of Bi atoms at this height as the first layer of Bi.

To enable further discussion of the structure of the film, the STM image is duplicated and a section of a Penrose P1 tiling of 2.50 nm edge length is overlaid on it in Fig. 2(d). Most of the pentagons and crescent shapes formed by Bi atoms are located at the vertices of the tiling. The vertices of the tiling are where cluster centres are located (protrusions of the clean surface). The Bi pentagonal stars of one orientation are located at the centre of the down-pentagons of the tiling. The pentagonal stars of the other orientation do not appear at specific sites of the tiling. The tiling and its decorations are expected

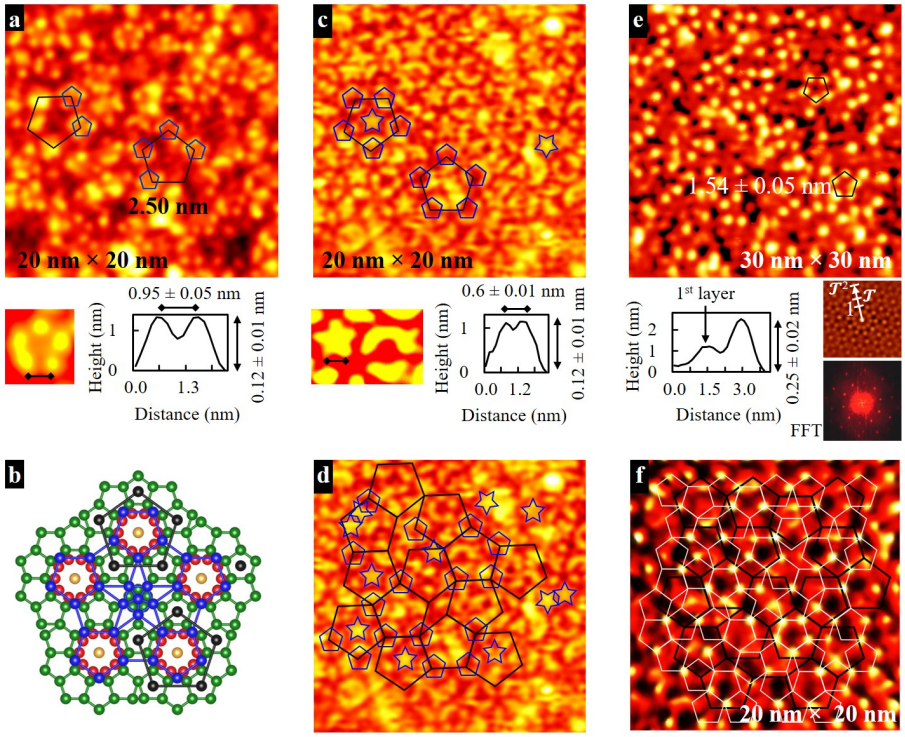

Figure 2: (a, c, e) STM images of the five-fold *i*-Ag-In-Yb surface after deposition of Bi for 5 minutes (a), 12 minutes (c) and 50 minutes (e). Pentagonal features are marked. Bottom of (a) and (c): highlighted regular features observed in STM and a line profile across the edge of the Bi pentagon (a) and the Bi star (c). Bottom of (e): line profile along an arbitrary direction in STM image (e) showing the height of the first and second layer Bi, and autocorrelation and fast Fourier transform of the STM image (e). Tunneling parameters (bias voltage, V_B and tunneling current, I_T): 2.0 V, 0.2 nA (a); -1.3 V, 0.1 nA (c); 1.7 V, 0.6 nA (e). (b) In-plane structure around the cluster centre demonstrating adsorption sites for first layer (blue) and second layer (black) Bi. The colour scheme and the scale are same as Fig. 1. Glue Yb atoms are also considered in this figure. Note that we have illustrated all ten Yb-pentagons around the cluster centre. However, in the real structure of the Yb sites may be unoccupied. (d) STM image (c) with a section of a Pentagonal P1 tiling overlaid. (f) A section of image (c) enhanced with FFT filtering with two sets of Penrose P1 tilings overlaid: the black tiling is related to the substrate and has an edge length of 2.50 nm and the white tiling maps the Bi layer and has 1.54 nm edge length.

from the substrate structure, which will be discussed in Section 4.

After deposition of Bi for 50 minutes, STM images show Bi pentagons of different height and size than the pentagons found at previous coverages. Fig. 2(e) is an STM image (30 nm $\times$ 30 nm) showing pentagons of Bi atoms with 1.54 ± 0.05 nm edge length. These pentagons are at a height of 0.25 ± 0.02 nm above the substrate (see the line profile given in Fig. 2(e), bottom), and we refer to these pentagons as 'second layer pentagons'. The pentagons of the second layer are inflated by τ with respect to first layer pentagons. These pentagons have two different orientations which are identical to the orientation of up- and down-pentagons of the substrate. From the size, orientation and location of the pentagons, the adsorption sites for the second layer are identified to be at the centre of Yb pentagons around the cluster centre. These sites are marked by red spheres in Fig. 2(b). The autocorrelation pattern together with the fast Fourier transform (FFT) of the image, shown in bottom of Fig. 2(e), display ten-fold symmetry which confirms the long-range quasicrystalline order of the film. The coverage of second layer Bi atoms is about 0.20 ML.

Fig. 2(f) shows a portion of STM image of Fig. 2(e) which is enhanced with FFT filtering. The second layer Bi atoms are located at the vertices of a Penrose P1 tiling of 1.54 nm edge length. The Penrose P1 tiling of 2.50 nm edge length (black tiling) of the substrate is also superimposed on the STM image. It can be noticed that the up-pentagons of tiling of the Bi layer are centred at the vertices of the substrate tiling. We will come back to this point in Section 4.

Further deposition of Bi yields three dimensional islands atop the quasicrystalline film. The structure of the islands could not be resolved by STM but the rectangular shape of the islands indicates a crystalline nature. Fig. 3(a) is a 420 nm $\times$ 420 nm STM image displaying rectangular Bi islands. The islands appear to grow from the step edges, which have lower coordination number compared to the centre of the terraces.

The islands have different orientations, as indicated by lines with different colours in Fig. 3(a). The orientation of the islands can be explained by analysing

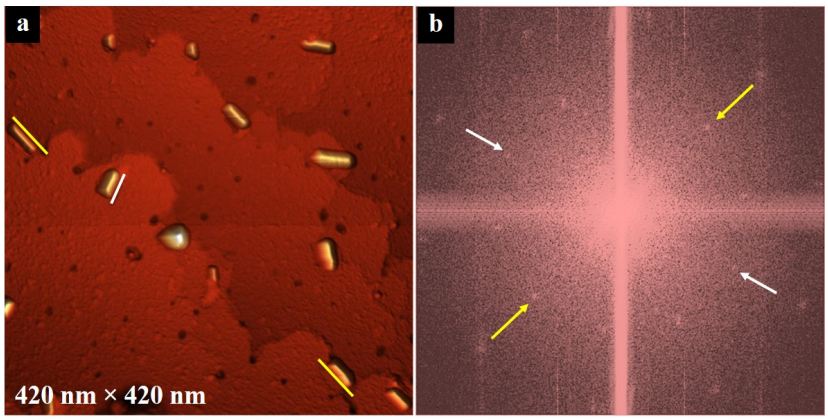

Figure 3: (a) STM image of the five-fold i-Ag-In-Yb surface after depositing Bi for 80 minutes, showing rectangular islands of different orientations. Bias voltage, $V_B = 2.7$ V, and tunneling current, $I_T = 0.2$ nA. (b) The FFT of image (a) showing decagonal rings which come from the quasicrystalline structure of the Bi monolayer.

the FFT of the STM images. The angles between the islands were found to be $2\pi/10$ which is consistent with the angle between high symmetry directions of the substrate. Fig. 3(b) is the FFT of the image 3(a), showing double decagonal rings (ten-fold symmetry) which result from the quasiperiodicity of the Bi film. The yellow and white arrows in the FFT image are the direction of Bi islands after rotation by 90°. Thus, the orientation of rectangular Bi islands appear to be parallel to high symmetry axes of the quasicrystalline film. This phenomenon was also observed when Bi was deposited on i-Al-Cu-Fe [20] and i-Al-Pd-Mn [21]. In the Bi/i-Al-Pd-Mn system, the rectangular islands transfer into hexagonal islands at certain coverage or flux, and these hexagonal islands are aligned along the high symmetry surface of the film [21]. There are also other systems, such as Pb/i-Ag-In-Yb, where islands are aligned parallel to the high symmetry axes of the substrate [36].

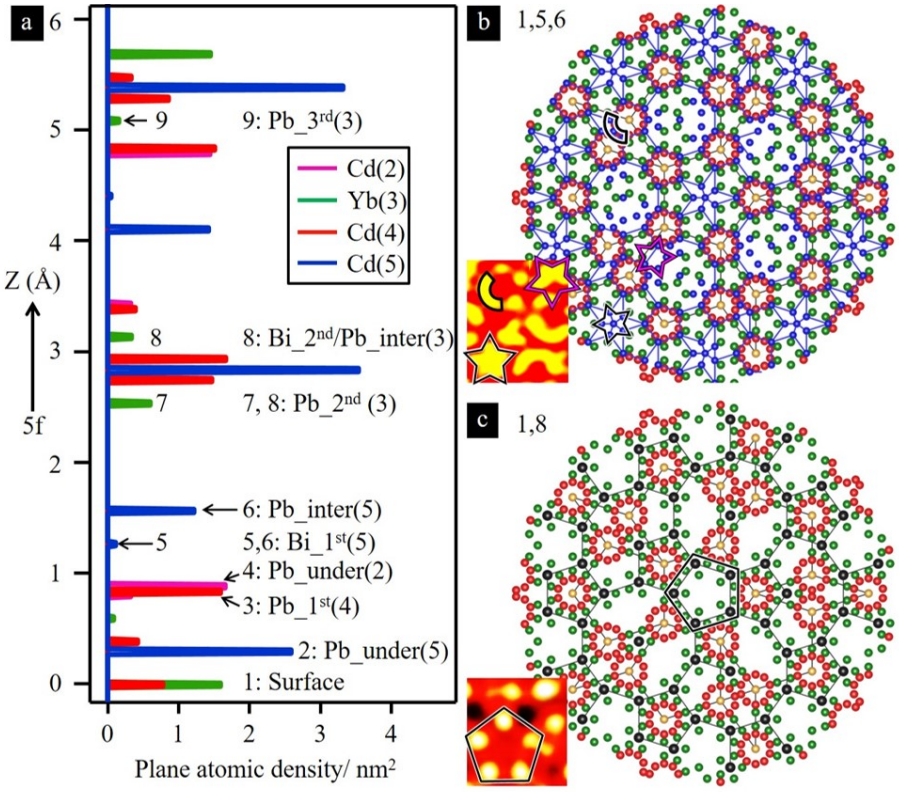

Figure 4: (a) Atomic density distribution of *i*-Ag-In-Yb quasicrystal along the five-fold direction. The density is estimated in slabs of 0.01 nm thickness. The planes where Pb and Bi layers are formed are indicated by different numbers. The number in parentheses indicates the n^{th} shell of the RTH cluster. (b) Structure of surface (plane 1) superimposed with planes 5 and 6, which explains the first layer of Bi. (c) Structure of surface (plane 1) superimposed with plane 8, which produces the second layer of Bi. The main motifs with STM are shown in the insets to compare with similar features produced in the model structure.

4. Discussion

To get further insight into the adsorption sites of Bi atoms, we analyse the structure of atomic planes of *i*-Ag-In-Yb forming the surface. Fig. 4(a) is the atomic density distribution of the planes along the five-fold direction. Different colours represent different atomic shells of the RTH clusters. Atomic planes which are relevant to the STM results are marked by numbers in Fig. 4(a). Plane 1 represents the surface plane, which intersects the centres of the RTH clusters. The structure of planes 5 and 6 is formed by atoms of the fifth shell of the cluster. The structure of these planes is superimposed with the surface plane in Fig. 4(b).

This structure produces pentagons of 0.96 nm edge length formed by atoms located in-between the Ag/In ring and Yb-rings. The pentagons are located at the vertices of the Penrose P1 tiling of the substrate. Similarly, a pentagonal star formed by six atoms (five atoms at the vertices of a pentagon of 0.59 nm edge length and an additional atom at the centre) can be found at the centre of the down-pentagons of the tiling of Bi. Both the size and location of the pentagons are consistent with STM results where we observed pentagons and stars of 0.95 ± 0.05 nm and 0.60 ± 0.01 nm edge length (Fig. 2(c)). In STM many of the stars were found to be incomplete and occasionally centre of star was missing. This can be explained if atomic sites of plane 5 are partially occupied. The pentagonal stars of the other orientation can also be related to the model structure. Pentagons of 0.59 nm edge length with other orientations (rotated by 36°) can be identified in plane 6. However, unlike the other pentagons, some vertices of these pentagons are unoccupied and centre atoms are missing. Nevertheless, adsorption of Bi atoms at these sites would yield an incomplete stars and an additional Bi atoms at unoccupied vertices and centre would make a star. The crescent features observed by STM can also be explained by the model structure. Additional atoms in-between the Ag/In- and Yb-rings would produce a crescent shape around the vertices of the tiling (an example is marked in Fig. 4(b)). The height of the first layer Bi atoms in the STM, 0.12 ± 0.01

nm, is also close to the separation between the surface and plane 5 (0.13 nm) or the separation between the surface and plane 6 (0.16 nm).

The structure of the second layer Bi can be explained by plane 8, which is formed by Yb atoms of the third shell of the RTH cluster. The structure of this plane superimposed with the substrate plane is shown in Fig. 4(c). Atoms of plane 8 lie at the centre of Yb pentagons of the surface surrounding the cluster centre. Here the colour of atoms of plane 8 have been changed from green to black so that they can be distinguished from Yb green atoms of the surface plane. The atoms of plane 8 form a Penrose P1 tiling of 1.56 nm edge length. The down-pentagons of this tiling are located at the vertices of the substrate tiling as observed in STM. The density of Bi atoms in the second layer, calculated by counting the number of atoms in the STM images divided by the area of the images, is 0.19 $\pm$ 0.01 atom/nm^2, which is close to the number of adsorption sites in plane 8 (0.22 site/nm^2). The height of Bi atoms in STM is 0.25 $\pm$ 0.02 nm, while the separation of plane 8 from surface plane 1 is 0.31 nm. This suggests that the second layer Bi is slightly relaxed towards the surface.

We now compare the results with Pb films deposited on the same substrate [12]. Like Bi, Pb atoms occupy the atomic sites of the RTH clusters [12], forming layers of different heights. However, the sequence of adsorption of layers is found to be different in the two systems. The previous study by combination of STM, XPS and DFT revealed that Pb atoms adsorb at five different heights [12]. These heights correspond to layers, which are formed at planes 3, 2/4, 6, 7/8 and 9 (Fig. 4(a)). These layers are specified as 1st, under, intermediate, second and third layers, respectively. The first layer is formed by Pb atoms adsorbed at the fourth shell of the RTH cluster (plane 3). After the formation of the first layer, an underlayer is formed, which is between the first Pb layer and the substrate. This layer is formed by Pb atoms adsorbed at the second and fifth shell of the RTH cluster. This layer was not observed by STM as it is formed after the first layer is completed, but the formation of this layer was confirmed by DFT and XPS. The sequence of adsorption for Pb is 'fourth shell (plane 3) $\rightarrow$ fifth shell (plane 2)/second shell (plane 4)$\rightarrow$ fifth shell (plane 6)$\rightarrow$ third shell

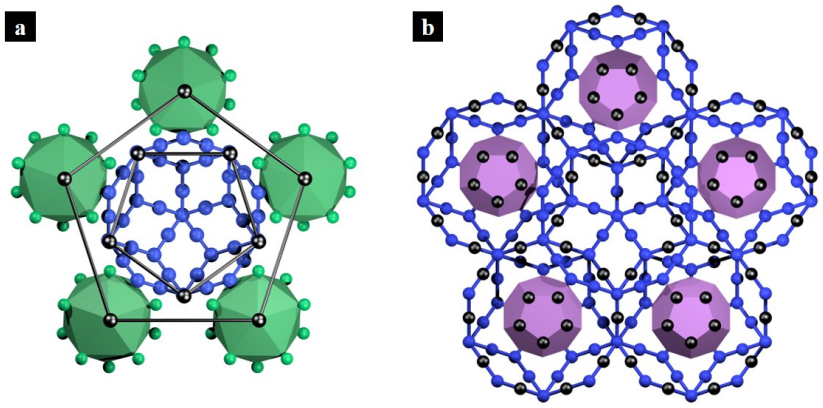

Figure 5: Surface truncated RTH clusters with Bi atoms atop, a view projected along the fivefold axis. Black spheres represent Bi atoms. Only relevant shells are shown for clarity. See text for further description how these clusters are constructed. (a) First and second layer Bi pentagons formed by the adatoms adsorbed at the fifth shell and third shell, respectively. (b) Bi atoms adsorbed at the second and fifth shell, which appear below the first layer. These adsorption sites are predicted by DFT [37].

(plane 7)→ third shell (plane 8)'.

The existence of the underlayer and intermediate layers is vital for the stability of the successive layers as the interatomic distance between the adsorbed Pb atoms in the same shell or layer is much larger than the nearest neighbour distance of Pb in its natural face-centred cubic structure. However, the distance between Pb atoms in different shells or layers is short enough (comparable to the fcc Pb-Pb distance) to have a strong interaction between the adatoms, stabilizing such 3D films.

The Bi first layer is formed at the fifth shell (plane 5 and 6), which is equivalent to the intermediate layer in Pb. Similarly, the second layer Pb is formed by the third shell (plane 7 and 8 in Fig. 4(a)), while only a specific set of third shell sites (layer 8) are occupied by Bi atoms. Density functional theory (DFT) calculations of initial stages of Bi growth on Ag-In-Yb have been reported by Nozawa *et al.* [37]. It has been shown that Bi is expected at plane 3 or 4 and plane 2. These sites are similar to the adsorption sites for the first and

underlayer of Pb. However, we did not identify this Bi layer in STM. Instead, we detected the first layer above these planes, i.e. at plane 5/6. It is possible that the layers predicted by DFT are formed only after the first layer is completed, in a similar way to the underlayer formed in Pb. Therefore, we suggest a sequence of adsorption for Bi to be 'fifth shell (plane 5 and 6) $\rightarrow$ fifth shell (plane 2) and/or fourth shell (plane 3) and/or second shell (plane 4) $\rightarrow$ third shell (plane 8)'. The DFT calculation has indicated that adsorption energies for Bi at plane 2 are close to that at plane and 3 or 4 (refer to [37] for adsorption energies). Therefore, these planes may be filled simultaneously.

Analysis of distances between the adatoms supports the formation of the Bi underlayers predicted by DFT. Fig. 5 shows surface truncated RTH clusters with Bi atoms atop. Six clusters are shown: five are located at the vertices of a pentagon of edge length 1.56 nm ($= 2.53$ nm$/\tau$) and the sixth is in the middle of the pentagon. The cluster in the middle is centred at the surface plane, while the centre of the other five are located at a plane 2.54 nm below the surface plane. This plane also yields a terrace observed in STM [34]. The nearest neighbour distances of Bi atoms in the same layer expected from the model structure are 0.6 nm (edge length of pentagonal stars of the first layer), 0.97 nm (edge length of pentagons of the first layer) and 1.56 nm (edge length of pentagons of the second layer). These distances are larger than the nearest neighbour distance of rhombohedral Bi, 0.45 nm [38]. However, the nearest neighbour distance of Bi atom in the first layer and substrate is 0.31 nm. Therefore, a Bi atom in the first layer is likely to interact with the substrate atoms, rather than with other adatoms in the first layer.

However, the second layer Bi atoms are 0.83 nm apart from the first layer and 0.6 nm from the substrate. Therefore, in order to stabilize the second layer, there must be Bi atoms adsorbed between the first layer and the substrate. If these atoms are adsorbed at the second shell (plane 4), the nearest neighbour distance between Bi atoms in the second layer and in this underlayer would be 0.34 nm. DFT has predicted a layer at plane 2 but also plane 3 or 4. However, a layer formed at plane 4 would not prevent the formation of another layer at

plane 2 or 3, because atomic sites on these planes are far enough apart to fit additional Bi atoms. Note that Pb also adsorbs at planes 2, 3 and 4.

The first layer Bi is observed after deposition for 12 minutes. With the same flux and deposition time for 50 minutes, we should observe four times more Bi than in the first layer. However, we detected only a fraction (the coverage of the second layer was only 0.2 ML). This could happen if the deposited Bi is used to form a layer below the first layer, or the sticking coefficient of Bi may decrease significantly after the first layer is formed. Further investigation is needed to clarify this.

5. Conclusions

The five-fold surface of *i*-Ag-In-Yb quasicrystal has been successfully used as a substrate to grow a quasicrystalline thin film of Bi. The growth was characterised by STM. The deposited Bi atoms occupy specific sites above the surface mimicing the structure of a three dimensional RTH cluster, the building block of the substrate. This result is in contrast with quasicrystalline Bi on Al-based quasicrystals, where quasicrystalline order is limited to a monolayer. Here, Bi forms layers of different heights above the substrate. Each layer is formed by Bi atoms adsorbed in a specific shell of the RTH cluster and there is an interaction between the atoms in different shells of the RTH cluster. The atoms at the same layer do not interact with each other as these atoms are far apart. However, they are likely to be bonded with atoms in other layers. Such an interaction between atoms in different layers is vital to stabilize the film. This result is the second such example after Pb/Ag-In-Yb, where a single element film displays quasicrystalline order in three-dimensions, i.e, quasicrystalline order is not limited to a monolayer but extend to other atomic layers. Following the formation of the quasicrystalline film, crystalline Bi islands were observed which are aligned along high symmetry axes of the substrate. Therefore, this system incorporates co-existence of crystalline and quasicrystalline allotropes of Bi, and thus provides the opportunity to simultaneously explore the influence

of crystalline and quasicrystalline order in physical properties.

This paper is submitted to the special issue "Surface Structure and Dynamics, in Honor of Karl-Heinz Rieder". When one of the authors (HRS) joined Karl-Heinz Rieder's research group in 1999 as a PhD student, the surface study of quasicrystals was in a preliminary stage, such that an observation of LEED patterns from a quasicrystal surface would be a major achievement. Through his encouragement and guidance, the group eventually reported the first quasicrystalline film of single elements using his favorite technique, helium atom scattering. This research topic has remained so fundamentally intriguing such that new types of quasicrystalline overlayers are still being pursued. The understanding of the topic reported in this paper builds on the foundations laid by him and his group.

Acknowledgment

This work was supported by the Engineering and Physical Sciences Research Council (grant number EP/D071828/1). KN is grateful for support in part by Grants-in-Aid for Scientific Research ((A) 15H02299 and (C) 17K05059) from the Ministry of Education, Culture, Sports, Science and Technology (MEXT) of Japan, and the Cooperative Research Program of "Network Joint Research Center for Materials and Devices".

References

[1] D. Shechtman, I. Blech, D. Gratias, J. W. Cahn, Metallic phase with long-range orientational order and no translational symmetry, Phys. Rev. Lett. 53 (20) (1984) 1951.

[2] X. Zeng, G. Ungar, Y. Liu, V. Percec, A. E. Dulcey, J. K. Hobbs, Supramolecular dendritic liquid quasicrystals, Nature 428 (6979) (2004) 157.

[3] A. Takano, W. Kawashima, A. Noro, Y. Isono, N. Tanaka, T. Dotera, Y. Matsushita, A mesoscopic archimedean tiling having a new complexity in an ABC star polymer, J. Polym. Sci. Polym. Phys. 43 (18) (2005) 2427.

[4] K. Hayashida, T. Dotera, A. Takano, Y. Matsushita, Polymeric quasicrystal: Mesoscopic quasicrystalline tiling in ABC star polymers, Phys. Rev. Lett. 98 (19) (2007) 195502.

[5] J. Mikhael, J. Roth, L. Helden, C. Bechinger, Archimedean-like tiling on decagonal quasicrystalline surfaces, Nature 454 (7203) (2008) 501.

[6] S. Fischer, A. Exner, K. Zielske, J. Perlich, S. Deloudi, W. Steurer, P. Lindner, S. Förster, Colloidal quasicrystals with 12-fold and 18-fold diffraction symmetry, Proceedings of the National Academy of Sciences 108 (5) (2011) 1810.

[7] S. Förster, K. Meinel, R. Hammer, M. Trautmann, W. Widdra, Quasicrystalline structure formation in a classical crystalline thin-film system, Nature 502 (7470) (2013) 215.

[8] V. Fournée, P. A. Thiel, New phenomena in epitaxial growth: solid films on quasicrystalline substrates, J. Phys. Appl. Phys. 38 (6) (2005) R83.

[9] H. R. Sharma, M. Shimoda, A. P. Tsai, Quasicrystal surfaces: structure and growth of atomic overlayers, Adv. Phys. 56 (3) (2007) 403.

[10] R. McGrath, J. A. Smerdon, H. R. Sharma, W. Theis, J. Ledieu, The surface science of quasicrystals, J. Phys.: Condens. Matter 22 (8) (2010) 084022.

[11] V. Fournée, J. Ledieu, M. Shimoda, M. Krajčí, H. R. Sharma, R. McGrath, Thin film growth on quasicrystalline surfaces, Isr. J. Chem. 51 (2011) 1.

[12] H. R. Sharma, K. Nozawa, J. A. Smerdon, P. J. Nugent, I. McLeod, V. R. Dhanak, M. Shimoda, Y. Ishii, A. P. Tsai, R. McGrath, Templated three-dimensional growth of quasicrystalline lead, Nat. Comm. 4 (2013) 2715.

[13] D. Gratias, F. Puyraimond, M. Quiquandon, A. Katz, Atomic clusters in icosahedral F-type quasicrystals, Phys. Rev. B 63 (2000) 024202.

[14] H. Takakura, C. P. Gómez, A. Yamamoto, M. de Boissieu, A. P. Tsai, Atomic structure of the binary icosahedral Yb–Cd quasicrystal, Nat. Mat. 6 (1) (2007) 58.

[15] K. J. Franke, H. R. Sharma, W. Theis, P. Gille, P. Ebert, K. H. Rieder, Quasicrystalline epitaxial single element monolayers on icosahedral Al-Pd-Mn and decagonal Al-Ni-Co quasicrystal surfaces, Phys. Rev. Lett. 89 (15) (2002) 156104.

[16] H. R. Sharma, M. Shimoda, A. R. Ross, T. A. Lograsso, A. P. Tsai, Real-space observation of quasicrystalline Sn monolayer formed on the fivefold surface of icosahedral Al-Cu-Fe quasicrystal, Phys. Rev. B 72 (4) (2005) 045428.

[17] J. Ledieu, L. Leung, L. H. Wearing, R. McGrath, T. A. Lograsso, D. Wu, V. Fournee, Self-assembly, structure, and electronic properties of a quasiperiodic lead monolayer, Phys. Rev. B 77 (7) (2008) 073409.

[18] J. A. Smerdon, J. K. Parle, L. H. Wearing, T. Lograsso, A. R. Ross, R. McGrath, Nucleation and growth of a quasicrystalline monolayer: Bi adsorption on the fivefold surface of i-$Al_{70}Pd_{21}Mn_9$, Phys. Rev. B 78 (7) (2008) 075407.

[19] V. Fournée, H. R. Sharma, M. Shimoda, A. P. Tsai, B. Unal, A. R. Ross, T. A. Lograsso, P. A. Thiel, Quantum size effects in metal thin films grown on quasicrystalline substrates, Phys. Rev. Lett. 95 (15) (2005) 155504.

[20] H. R. Sharma, V. Fournée, M. Shimoda, A. R. Ross, T. A. Lograsso, P. Gille, A. P. Tsai, Growth of Bi thin films on quasicrystal surfaces, Phys. Rev. B 78 (15) (2008) 155416.

[21] J. A. Smerdon, N. Cross, V. R. Dhanak, H. R. Sharma, K. M. Young, T. A. Lograsso, A. R. Ross, R. McGrath, Structure and reactivity of Bi

allotropes on the fivefold icosahedral Al–Pd–Mn quasicrystal surface, J. Phys.: Condensed Matter 22 (34) (2010) 345002.

[22] J. Ledieu, J. T. Hoeft, D. E. Reid, J. A. Smerdon, R. D. Diehl, T. A. Lograsso, A. R. Ross, R. McGrath, Pseudomorphic growth of a single element quasiperiodic ultrathin film on a quasicrystal substrate, Phys. Rev. Lett. 92 (13) (2004) 135507.

[23] J. A. Smerdon, J. Ledieu, J. T. Hoeft, D. E. Reid, L. H. Wearing, R. D. Diehl, T. A. Lograsso, A. R. Ross, R. McGrath, Adsorption of cobalt on the tenfold surface of d-$Al_{72}Ni_{11}Co_{17}$ and on the fivefold surface of i-$Al_{70}Pd_{21}Mn_9$, Phil. Mag. 86 (6-8) (2006) 841.

[24] K. Pussi, M. Gierer, R. D. Diehl, The uniaxially aperiodic structure of a thin Cu film on fivefold i-AlPdMn, J. Phys.: Condensed Matter 21 (47) (2009) 474213.

[25] T. Cai, J. Ledieu, R. McGrath, V. Fournée, T. Lograsso, A. Ross, P. Thiel, Pseudomorphic starfish: nucleation of extrinsic metal atoms on a quasicrystalline substrate, Surf. Sci. 526 (1) (2003) 115.

[26] J. Ledieu, P. Unsworth, T. A. Lograsso, A. R. Ross, R. McGrath, Ordering of Si atoms on the fivefold Al-Pd-Mn quasicrystal surface, Phys. Rev. B 73 (1) (2006) 012204.

[27] M. Krajčí, J. Hafner, Ab initio study of quasiperiodic monolayers on a fivefold i-Al-Pd-Mn surface, Phys. Rev. B 71 (18) (2005) 184207.

[28] H. R. Sharma, J. Ledieu, V. Fournée, P. Gille, Influence of the substrate temperature and deposition flux in the growth of a Bi thin film on the ten-fold decagonal Al-Ni-Co surface, Phil. Mag. 91 (19-21) (2011) 2870.

[29] B. Ünal, V. Fournée, P. A. Thiel, J. W. Evans, Structure and growth of height-selected Ag islands on fivefold i-AlPdMn quasicrystalline surfaces: STM analysis and step dynamics modeling, Phys. Rev. Lett. 102 (2009) 196103.

[30] J. Ledieu, J. T. Hoeft, D. E. Reid, J. A. Smerdon, R. D. Diehl, N. Ferralis, T. A. Lograsso, A. R. Ross, R. McGrath, Copper adsorption on the fivefold $Al_{70}Pd_{21}Mn_9$ quasicrystal surface, Phys. Rev. B 72 (3) (2005) 035420.

[31] J. A. Smerdon, J. Ledieu, R. McGrath, T. C. Q. Noakes, P. Bailey, M. Draxler, C. F. McConville, T. A. Lograsso, A. R. Ross, Characterization of aperiodic and periodic thin Cu films formed on the five-fold surface of i-$Al_{70}Pd_{21}Mn_9$, Phys. Rev. B (3) 035429.

[32] H. R. Sharma, M. Shimoda, S. Ohhashi, A. P. Tsai, First UHV surface studies of single-grain icosahedral Ag-In-Yb quasicrystal, Phil. Mag. 87 (18-21) (2007) 2989–2994.

[33] B. Ünal, C. J. Jenks, P. A. Thiel, Comparison between experimental surface data and bulk structure models for quasicrystalline AlPdMn: Average atomic densities and chemical compositions, Phys. Rev. B 77 (2008) 195419.

[34] H. R. Sharma, M. Shimoda, K. Sagisaka, H. Takakura, J. A. Smerdon, P. J. Nugent, R. McGrath, D. Fujita, S. Ohhashi, A. P. Tsai, Structure of the fivefold surface of the Ag-In-Yb icosahedral quasicrystal, Phys. Rev. B 80 (12) (2009) 121401.

[35] P. J. Nugent, J. Smerdon, R. McGrath, M. Shimoda, C. Cui, A. P. Tsai, H. R. Sharma, Step-terrace morphology and reactivity to C_{60} of the fivefold i-Ag-In-Yb surface, Phil. Mag. 91 (2010) 2862.

[36] H. R. Sharma, J. A. Smerdon, P. J. Nugent, A. Ribeiro, I. McLeod, V. R. Dhanak, M. Shimoda, A. P. Tsai, R. McGrath, Crystalline and quasicrystalline allotropes of Pb formed on the fivefold surface of icosahedral Ag-In-Yb, J. Chem. Phys. 140 (17) (2014) 174710.

[37] K. Nozawa, Y. Ishii, Adsorption structure of Bi on the fivefold surface of i-Ag-In-Yb quasicrystal, J. Phys.: Conference Series 809 (1) (2017) 012018.

[38] P. Hofmann, The surfaces of bismuth: Structural and electronic properties, Prog. Surf. Sci. 81 (5) (2006) 191.